THE ASTROPHYSICAL JOURNAL, 436:L9–L13, 1994 November 20

MULTIWAVELENGTH OBSERVATIONS OF HERCULES X-1/HZ HERCULIS

S. D. VRTILEK,[1,2] T. MIHARA,[3] F. A. PRIMINI,[1] P. KAHABKA,[4] H. MARSHALL,[5] F. AGERER,[6] P. A. CHARLES,[7] F. H. CHENG,[2] K. DENNERL,[4] C. LA DOUS,[8] E. M. HU,[9] R. RUTTEN,[10] P. SERLEMITSOS,[11] Y. SOONG,[11] J. STULL,[12] J. TRÜMPER,[4] W. VOGES,[4] R. M. WAGNER,[13] AND R. WILSON[14]

Received 1994 June 8; accepted 1994 August 20

ABSTRACT

We present first results from a multiwavelength campaign to observe the binary pulsar system Her X-1/HZ Her. The campaign spanned 4 days during 1993 August: observations were taken with five satellites (*IUE*, *EUVE*, *ROSAT*, *ASCA*, and *CGRO*/BATSE) and several ground-based facilities. A substantial, unexpected drop in flux at X-ray energies, with no change in absorbing column density, was observed. The pulse period has increased from the previous measurement, contrary to the usual spin-up, and no pulsed emission is detected above 0.9 keV in the low state. The optical and UV fluxes continued to show 1.7 day modulation attributed to X-ray heating of the companion star. However, the significant reduction in UV flux observed around eclipse implies an absence of the normally observed excess attributed to X-ray heating of the disk. We conclude that we have observed an anomalous low state, seen only once before (Parmar et al. 1985), in which the X-ray flux is not redistributed but obscured. We suggest explanations for the behavior of the flux at different wavelengths.

Subject headings: accretion, accretion disks — pulsars: individual (Hercules X-1)

1. INTRODUCTION

The availability of several space-borne astronomical observatories offers a unique opportunity for study of the Her X-1/HZ Her system. In particular, the *EUVE* makes possible for the first time observations of Her X-1 in the lower energy range of its strong soft component (McCray et al. 1982; Vrtilek & Halpern 1985). Several X-ray pulsars show this component, but, owing to the high Galactic latitude and correspondingly low interstellar absorption toward Her X-1, it is the *only* X-ray binary system that *EUVE* is able to study. By complementing the *EUVE* observations with simultaneous coverage in several wave bands, we are able to obtain a comprehensive view of emission from ionized material in several environments ranging from the inner edge of the accretion disk to the magnetosphere and corona. The observations allow study of the highly variable continuum as well as line emission from He II and C IV (optical and *IUE*), Fe XVIII–XXII (*EUVE*), and Fe L-shell and K-shell features (*ROSAT* and *ASCA*).

[1] Center for Astrophysics, 60 Garden Street, Cambridge, MA 02138.
[2] Department of Astronomy, University of Maryland, College Park, MD 20742.
[3] Institute of Physical and Chemical Research (RIKEN), 2-1 Hirosawa, Wako, Saitama 351-01, Japan.
[4] Max-Planck-Institut für Extraterrestrische Physik, D-85740 Garching bei München, Germany.
[5] Eureka Scientific, Inc., 2452 Delmer Street, Oakland, CA 94602.
[6] Dorfstrasse 19, D-84184 Zweikirchen, Germany.
[7] Department of Physics, Oxford University, Oxford OX1 3RH, UK.
[8] ESA/*IUE*, Villafranca, Apartado 50727, 28080 Madrid, Spain.
[9] Institute for Astronomy, 2680 Woodlawn Drive, Honolulu, HI 96822.
[10] Royal Greenwich Observatory/NFRA, E-38780 la Palma, Islas Canarias, Spain.
[11] NASA/GSFC, LHEA, Code 666, Greenbelt, MD 20771.
[12] Alfred University, 26 North Main Street, Alfred, NY 14802.
[13] Department of Astronomy, Ohio State University, Columbus, OH 43210.
[14] NASA/MSFC, Code ES-84, Huntsville, AL 35812.

2. OBSERVATIONS

The observed light curves are plotted in Figure 1. The *EUVE* observations took place over 4 days during the main-on state of the 35 day cycle (ϕ_{35}^0 = JD 2,448,961.3 and P_{35} = 34.875 [Wilson et al. 1993]). Averaged over the 4 days, BATSE measured an intensity of ~25% of the expected value for the main-on state, as determined from BATSE observation during the previous 3 years (Wilson et al. 1993). Source intensities in the preceding and succeeding 35 day cycles were ~50% and ~33% of the expected values, respectively. The *ASCA* measured flux of 1.5 mCrab was a factor of 50 below the expected value, as determined from *EXOSAT* observations during identical 35 day and binary phases. Two weeks later, during the 35 day short-on state, *ASCA* again found the source a factor of 50 below the expected value (Mihara & Soong 1994). Count rates determined by *ROSAT* on the first day (peak of main-on state) were a factor of 2 below the count rate predicted from *ROSAT* all-sky survey short-on state data (Mavromatakis 1993). The *ROSAT* count rate ultimately dropped by a factor of 40 on the third day and 35 days later continued at the anomalous low rate. The *EUVE* Deep Survey count rates showed a time dependence similar to that of *ROSAT*. The *IUE* continuum continued to show the 1.7 day variations found in previous *IUE* observations for the *same* 35 day phase (Howarth & Wilson 1993), with the exception of a significant decrease from the expected flux near eclipse. The optical observations, to the extent that coverage was available, showed no deviation from the expected behavior (Petro & Hiltner 1976).

The X-ray spectra were extracted from three intervals which are identified on Figure 1 and Table 1. The intervals represent the highest observed count rates (about one-half that expected during a normal "main-on" state, INT 1), the "anomalous low" state (INT 3), and an intermediate state (INT 2). All *ROSAT* data were well fitted by a blackbody (BB) plus power law (PL) model. There is no increase in absorbing column

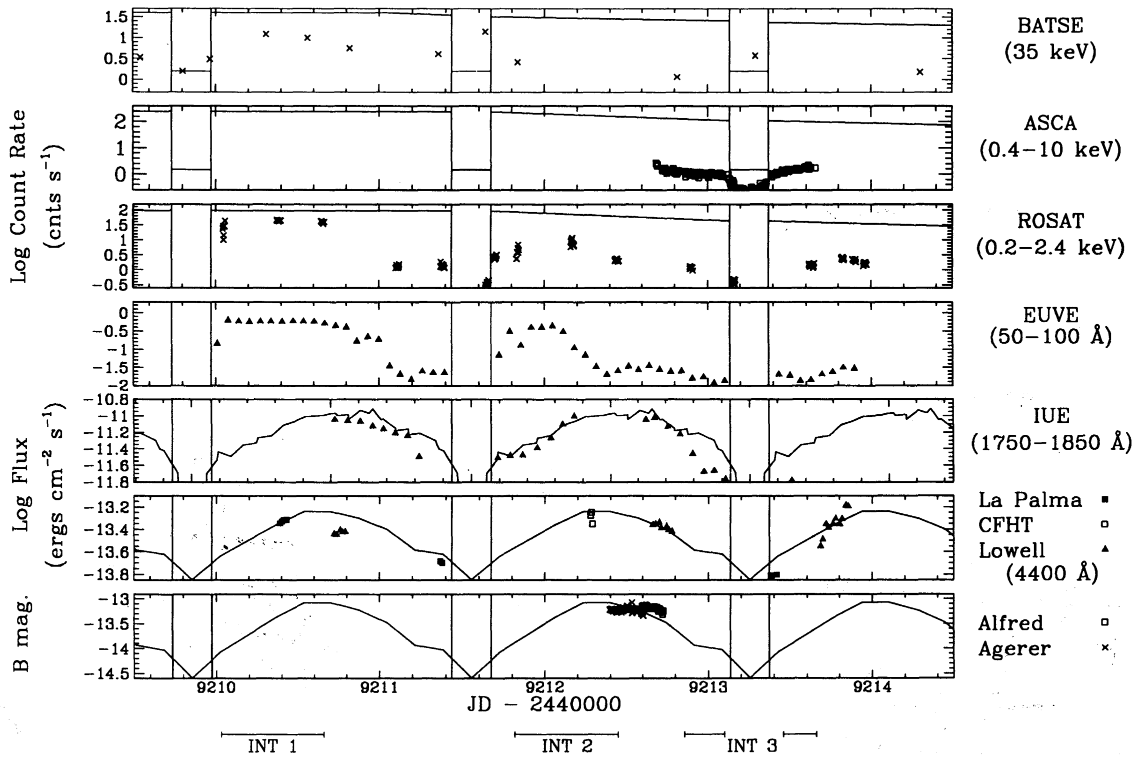

FIG. 1.—Light curves, with the count rates plotted on a logarithmic ordinate scale. The vertical lines delimit the expected times of X-ray eclipses for the 2–6 keV energy band ($\phi^0_{\rm orb}$ = eclipse center = JD 2,442,859.726688 and $P_{\rm orb}$ = 1.700167788 days [Deeter et al. 1991]). The smooth curves designate the expected value as determined from behavior in earlier observations.

density from INT 1 to INT 3, and the measured column density in all three intervals is consistent with interstellar absorption to the source. The PL index for INT 1 is somewhat steeper than that measured with *EXOSAT* during the main-on state ($\alpha = 1.1$–1.4), but the indices for INT 2 and 3 were comparable to that measured during the extended low state ($\alpha = 0.5$; Parmar et al. 1985). The BB-emitting radii inferred during INT 1, 2, and 3 are factors of 2, 3, and 10, respectively, below those measured by Vrtilek & Halpern (1985) during a normal main-on state. A BB and two PLs were fitted to the

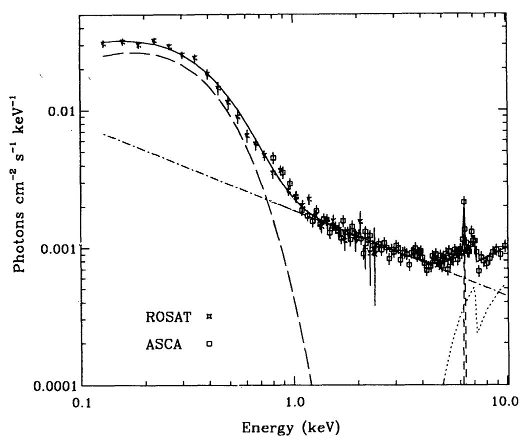

FIG. 2.—Combined spectral fits to the *ROSAT* and *ASCA* data during INT 3 (see § 2 and Fig. 1). One sigma error bars are plotted on the points. The smooth curve is the best-fit model as listed in Table 1. The dotted line is the absorbed PL. The long dashed line is the BB. The dot-dashed line is the unabsorbed PL. The short-dashed line is the Fe K-shell line.

ASCA GIS data. The PL indices are consistent with those measured during the extended low state observed by Parmar et al. 1985 ($\alpha = 0.5$). The BB radius is comparable to that measured by *ROSAT* in INT 3. A combined fit to the *ASCA* and *ROSAT* observations for INT 3 is plotted in Figure 2. The *EUVE* short-wavelength spectrometer detected continuum emission during INT 1 and INT 2, but only upper limits were obtained during INT 3. A BB fixed at a temperature of 0.09 keV (the *ROSAT* value) provides a good fit to INT 1.

In Figure 3 we have plotted the energy flux versus frequency for INT 1 and INT 3. For INT 1 the 0.3–10 keV "expected" spectrum is taken from Vrtilek & Halpern (1985). Her X-1/HZ Her displays a fairly flat spectrum across four orders of magnitude in frequency during the "normal" main-on state. The reduction in X-ray flux in the "anomalous" low state does not appear to be associated with an increase in flux in some other portion of the observed frequency space.

Mihara et al. (1991), using *Ginga* observations, determined a Fe Kα equivalent width (EW) of 900 ± 90 eV during the normal quiescent state and 240 ± 90 eV during the main-on state of Her X-1. The corresponding continuum intensities are 4 and 110 mcrab. Thus, the continuum intensity is reduced by a factor of $\sim$25 and the EW increased by a factor of $\sim$4 in the quiescent state. This behavior suggests that the line emission comprises two components, one originating near the central (pulsed) source, and the other in a diffuse accretion disk corona (ADC). *EXOSAT* observations (Vrtilek et al. 1994) suggest that $\sim$50% of the total line emission originates in the ADC. Intensities of 95 mcrab and 15 mcrab for the pulsed and ADC components in the main-on state, with all of the pulsed emission and $\sim$75% of the ADC emission absent in the quiescent state, can explain both these results.

TABLE 1

SPECTRAL FITS TO X-RAY OBSERVATIONS

TIME JD −2,449,200	BLACKBODY[a] A_{BB} (cm^{-2} s^{-1} keV^{-1})	BLACKBODY[a] kT (keV)	POWER LAW 1[b] A_{PL1} (cm^{-2} s^{-1} keV^{-1})	POWER LAW 1[b] α1	POWER LAW 1[b] log N_H (cm^{-2})	POWER LAW 2[b] A_{PL2} (cm^{-2} s^{-1} keV^{-1})	POWER LAW 2[b] α2	POWER LAW 2[b] log N_H (cm^{-2})	χ^2_ν
				ROSAT					
10.03–10.66	110.0	0.09 ± 0.003	...	...	...	5.47E−2	1.76	19.5 ± 0.1	2.4
11.82–12.45	34.2	0.09 ± 0.003	...	...	...	9.25E−3	0.60[c]	19.0 ± 0.2	1.1
12.86–13.10 + 13.46–13.66	3.5	0.11 ± 0.005	...	...	...	1.92E − 3	0.60[c]	19.0 ± 0.2	0.9
				ASCA GIS[d]					
12.86–13.10 + 13.46–13.66	8.4 ± 2.5	0.11[e]	(5 ± 2)E − 3	0.55 ± 0.07	23.96 ± 0.14	(1.7 ± 0.1)E − 3	0.55	<21.5	0.9
				ROSAT + *ASCA* GIS2[f]					
12.86–13.10 + 13.46–13.66	3.28 ± 0.25	0.11 ± 0.00	(5 ± 2)E − 3	0.63 ± 0.06	23.91 ± 0.12	(1.9 ± 0.1)E − 3	0.63	<19.2	1.0

[a] $N(E)(\mathrm{cm^{-2}\ s^{-1}\ keV^{-1}}) = (A_{BB}E^2)[(e^{E/kT} - 1)]^{-1}\ [e^{-N_H\sigma(E)}]$; A_{BB} is the normalization constant, E is the photon energy in keV, T is the temperature in kelvins, k is the Boltzmann constant, N_H is the column density, and $\sigma(E)$ is the photoelectric absorption cross section obtained by considering the effect of all the heavy elements at their cosmic abundances as defined by Morrison & McCammon 1983.

[b] $N(E)(\mathrm{cm^{-2}\ s^{-1}\ keV^{-1}}) = (A_{PL}E^{-\alpha})[e^{-N_H\sigma(E)}]$; A_{PL} is the normalization constant; α is a power-law index.

[c] The photon index α is fixed at the *ASCA* value.

[d] The photon index α is common for PL1 and PL2. *ASCA* fit also required a line at 6.31 ± 0.1 keV with an equivalent width of 90 ± 30 eV.

[e] The blackbody temperature is held fixed at the *ROSAT* value.

[f] The photon index α is common for PL1 and PL2.

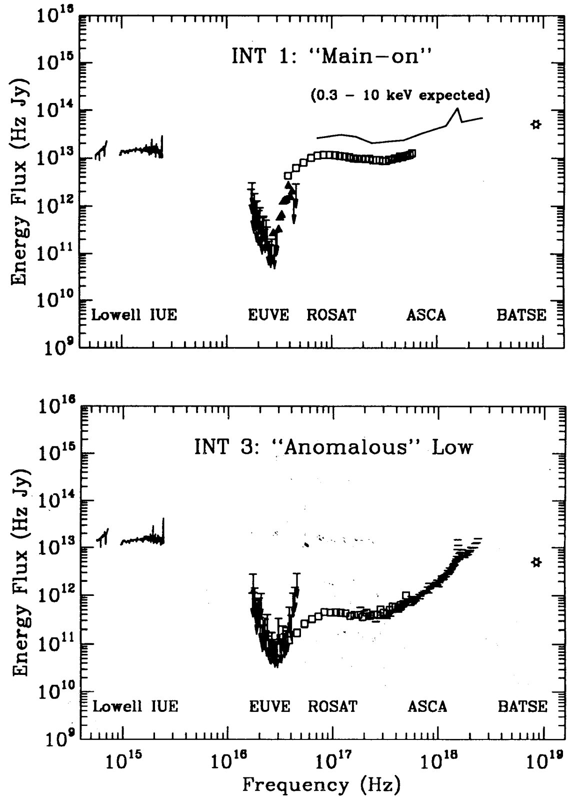

FIG. 3.—Log νF_ν vs. log ν for INT 1 and INT 3. For the optical and *IUE* bands, spectra are used that are as close to the same binary phase (0.4) as possible.

During our observation of the anomalous low state, the *ASCA* GIS detected Fe K-shell emission at 6.3 ± 0.1 keV with an EW of 90 ± 30 eV and a weak K absorption edge at 7.2 keV. This EW is reduced by a factor of 10 from the value in the quiescent state. In the context of our model for X-ray propagation through an ADC (Vrtilek, Soker, & Raymond 1993) the lack of a strong K edge and small EW in the anomalous low state imply an inclination angle of $\sim 70°$, or a shift of $\sim 10°$ from the "normal" inclination (Nagase 1989; Vrtilek et al. 1993).

The *ASCA* SIS detected lines around 0.9 and 1.0 keV attributable to Fe L-shell emission with EWs roughly 1/10 that of the K-shell emission (Mihara & Soong 1994). The lines of Fe XVIII–XXII expected in the 70–100 Å range were not observed by *EUVE*. Limits on line emission in the *EUVE* energy range will be presented by Marshall et al. (1994). The *IUE* detected emission lines from N V (1240 Å), C IV (1540 Å), and He II (1640 Å). N V shows a stronger dependence on binary phase then either C IV or He II, in concurrence with earlier observations (Gursky et al. 1980). Detailed modeling of the UV lines produced by X-ray heating of the accretion disk and companion star will be presented by Vrtilek et al. (1994).

ROSAT measured a pulse period of 1.237749 (1) s during INT 1; this is an *increase* (7 μs) from the previous measurement (Deeter et al. 1991), contrary to the usual spin-up. The pulse profile and energy dependence show the normal main-on state behavior during INT 1: the shift of pulse phase by ~ 0.5 around 0.9 keV is clearly detected. The pulsed fraction ([maximum counts—minimum counts]/[mean counts]) is 62%, 49%, and 26% for the 0.1–0.4 keV, 0.5–0.9 keV, and 0.9–2.5 keV bands. During INT 3 a triangle-like pulse with pulsed fraction of about 24% is detected for the energy range 0.1–0.4 keV, weak pulsation is seen at 0.5–0.9 keV, and no pulsations are seen at 0.9–2.5 keV. The *EUVE* deep survey data show a periodic signal at 1.2377475(10) s with a pulsed fraction of 52% $\pm$ 1% during INT 1. *ASCA* confirms the lack of pulsed emission above 0.9 keV, with an upper limit of 1.5% for the amplitude of a sinusoidal modulation.

3. SUMMARY AND CONCLUSIONS

A sharp decrease in medium-energy X-ray flux with little or no apparent change in optical and UV flux has been detected once before in Her X-1. The increase in pulse period and lack of pulsations at energies greater than 1 keV during the low state were also observed (Parmar et al. 1985; Mihara et al. 1991; Sheffer et al. 1992). However, during the previous extended low state, no UV observations were obtained for the binary phase near eclipse, where we see a significant decrease in UV flux (Boyle et al. 1988).

Observations of 20 35-day episodes by BATSE, leading up to and including the campaign interval, suggest that the hard X-ray flux of Her X-1 undergoes episodes of reduction that are correlated with spin-down. The correlation between times of low hard X-ray luminosity and episodes of spin-down are predicted by models such as those of Ghosh & Lamb (1979); an *increase* in the mass accretion rate causes the Alfvén radius at which material joins the magnetosphere to move in, *reducing* the drag-producing torques of the field lines threading the disk outside the corotation radius, leading to spin-up (Wilson et al. 1993). Correlations between drop in X-ray flux and a switch-over from spin-up to spin-down have also been observed in the binary pulsars GX 1+4 (Makishima et al. 1988; Sakao et al. 1990) and LMC X-4 (Dennerl 1991).

The model used for our spectral fits had first been applied to spectra of Her X-1 during dips by Vrtilek & Halpern (1985) and by Sheffer et al. (1992) for the extended low state observed in 1983. Sheffer et al. (1992) interpreted the absorbed PL as X-rays reflected from the atmosphere of the normal star and the unabsorbed PL as X-rays scattered from a high-temperature corona. This interpretation provides for blocking of the direct, pulsed emission while some hard X-rays continue to be observed; the hard X-rays are "reflected" from the companion's atmosphere so that energy stays the same, but the pulse information is lost.

We suggest that the initial drop in count rate accompanied by a change from spin-up to spin-down (as inferred from BATSE observations) corresponds to a reduction in accretion rate; the change in torque on the neutron star implied by the switch from spin-up to spin-down then acts to shift the disk into the line of sight (the timescale for changes to the disk is presumably the time for viscous dissipation in the disk, roughly 1 month for the Her X-1/HZ Her system). Such a disk shift is also implied by our interpretation of the iron K-shell intensity (§ 2). The decrease in accretion rate is insufficient to account for the drop in flux, so disk obscuration must be taking place. All of the pulsed emission and some of the emission from the extended corona gets obscured. In this context the *ROSAT* spectra for INT 1 show a PL that is due partly to direct pulsed emission which swamps the PL component owing to scattering from the ADC. The BB component is due to reprocessed hard X-rays (from the same ADC or perhaps from a larger corona extending to the Alfvén radius). For INT 2 the direct pulsed emission is much reduced, allowing the spectrum reflected from the ADC to be detected. For INT 3 the direct pulsed emission is completely gone, and the PL contribution is only the spectrum reflected from the ADC. The BB component from reprocessed hard X-rays is reduced by a factor of 10. In the *ASCA* observations the direct, pulsed emission is missing, and the "absorbed" PL represent an additional component due to reflection from the normal star. The overall *ASCA* flux is reduced somewhat more than the *ROSAT* flux because a larger percentage of the *ASCA* flux is due to the direct pulsed emission that has been obscured.

The optical emission, which is dominated by X-ray heating of the companion star, is unaffected. The UV variations are affected by the disk being in the line of sight to the extent that the component of UV emission due to X-ray heating of the disk is missing.

This *Letter* constitutes a preliminary summary of an extensive multiwavelength campaign on the intriguing binary pulsar system Her X-1/Hz Her. The *simultaneous* wavelength coverage from 0.001 to 35 keV is useful in determining the energy balance of the system. The ability to separate the hot inner parts of the accretion disk (soft X-rays and far-UV) and its cool outer regions (optical and near-UV) puts constraints on the structure and dynamics of the accretion disk. The broadband coverage is particularly beneficial to the study of line emission, since it puts stringent constraints on the continuum. Comprehensive modeling efforts that utilize the large body of data gathered are currently underway (Vrtilek et al. 1994; Marshall et al. 1994; Primini et al. 1994; Kahabka et al. 1994; Mihara et al. 1994).

S. D. V., F. H. C., and F. A. P. were supported by NASA grants NAGW-2685, NAG 5-2374, and NAG 5-2429 and by a NSF VPW grant.

REFERENCES

Boyle, S. J., Howarth, I. D., Wilson, R., & Raymond, J. C. 1988, Adv. Space Res., 8, 509

Deeter, J. E., Boynton, P. E., Miyamoto, S., Kitamoto, S., Nagase, F., & Kawai, N. 1991, ApJ, 383, 324

Dennerl, K. 1991, Ph.D. thesis, Univ. München; also MPE Rept., 232

Ghosh, P., & Lamb, F. K. 1979, ApJ, 234, 296

Gursky, H. B., et al. 1980, ApJ, 237, 1163

Howarth, I. D., & Wilson, B. 1983, MNRAS, 202, 347

Kahabka, P., et al. 1994, in preparation

Makishima, K., Ohashi, T., Sakao, T., Dotani, T., Inoue, H., Thomas, H. D., Turner, M. J. L., Kii, T., & Tawara, Y. 1988, Nature, 333, 746

Marshall, H. W., et al. 1994, in preparation

Mavromatakis, F. 1993, A&A, 273, 147

McCray, R. A., Shull, J. M., Boynton, P. E., Deeter, J. E., Holt, S. S., & White, N. E. 1982, ApJ, 262, 301

Mihara, T., et al. 1994, in preparation

Mihara, T., Ohashi, T., Makishima, K., Nagase, F., Kitamoto, S., & Koyama, K. 1991, PASJ, 54, 501

Mihara, T., & Soong, Y. in Proc. of New Horizon of X-ray Astronomy, ed. F. Makino (Tokyo: Universal Academy), in press

Morrison, R., & McCammon, D. 1983, ApJ, 270, 119

Nagase, F. 1989, in Proc. of the 23d ESLAB Symp. on Two Topics in X-Ray Astronomy, ed. J. Hunt & B. Battrick (Paris: ESA), 47

Parmar, A. N., Pietsch, W., McKechnie, S., White, N. E., Trümper, J., Voges, W., & Barr, P. 1985, Nature, 313, 119

Petro, L., & Hiltner, W. A. 1976, ApJ, 181, L39

Primini, F. A., et al. 1994, in preparation

Sakao, T., et al. 1990, MNRAS, 246, 11P

Sheffer, E. K., et al. 1992, Astron. Zh., 69, 82

Vrtilek, S. D., et al. 1994, in preparation

Vrtilek, S. D., & Halpern, J. P. 1985, ApJ, 296, 606

Vrtilek, S. D., Soker, N., & Raymond, J. C. 1993, ApJ, 404, 696

Wilson, R. B., Finger, M. H., Pendleton, G. N., Briggs, M., & Bildsten, L. 1993, in The Evolution of X-Ray Binaries, ed. S. Holt (New York: AIP), 475